ELSEVIER

Pattern Recognition Letters 23 (2002) 1095–1102

Pattern Recognition Letters

www.elsevier.com/locate/patrec

Texture classification using Gabor filters

Mahamadou Idrissa *[,1], Marc Acheroy

Royal Military Academy, Signal and Image Centre, Avenue de la Renaissance 30, B-1000 Brussels, Belgium

Abstract

An unsupervised texture classification scheme is proposed in this paper. The texture features are based on the image local spectrum which is obtained by a bank of Gabor filters. The fuzzy clustering algorithm is used for unsupervised classification. In many applications, this algorithm depends on assumptions made about the number of subgroups present in the data. Therefore we discuss ideas behind cluster validity measures and propose a method for choosing the optimal number of clusters.

Keywords: Gabor filters; Classification; Fuzzy clustering; Cluster validity

1. Introduction

In satellite image interpretation, classification is the operation by which an operator would like to detect different kinds of region like forest, urban zone, waterways, etc. As the scene is a set of points (pixels) with intensity in grey scale values in several bands, most methods use these grey scale values to determine the kind of terrain. However, a single ground cover usually occupies a number of pixels with some variability in their grey scale values. A more satisfactory interpretation of the scene should thus include textural aspects of regions.

In general, texture is characterized by invariance of certain local attributes that are periodically or quasi-periodically distributed over a region. There are many approaches for analyzing image texture. Haralick (1979) proposed a set of features (energy, entropy, maximum probability, correlation, etc.) based on grey level cooccurrence matrices. Some statistical techniques use Markov Random Field models to characterize textures (Cross and Jain, 1983). The spectral approach (Bovik et al., 1990; Randen and Husoy, 1999) to texture analysis is referred to as the multi-channel filtering approach. Textures are characterized by their responses to filters, each one being selective in spatial frequency and orientation.

In this paper, we present a spectral approach to extract texture features. The textured input image is decomposed into feature images using a bank of Gabor filters. These feature images are used to form feature vectors and each of them

* Corresponding author. Tel.: +32-2-737-64-74; fax: +32-2-737-64-72.

E-mail addresses: idrissa@elec.rma.ac.be (M. Idrissa), acheroy@elec.rma.ac.be (M. Acheroy).

[1] The first author's research is funded by the HUDEM project: HUDEM (HUmanitarian DEMining) is a technology exploration project on humanitarian demining launched by the Belgian Minister of Defense with funding provided by his Department, the Ministry of Foreign Affairs and the State Secretariat for Development Aid.

0167-8655/02/$ - see front matter
PII: S0167-8655(02)00056-9

corresponds to one dimension of the feature space. Then, we present the Fuzzy c-means clustering algorithm used for unsupervised classification of the input pixels based on their associated feature vector. This method considers clusters as fuzzy sets, while membership function measures the possibility that each feature vector belongs to a cluster. At last, we present methods for evaluating how well different textures are separated in feature space, as well as measuring classification performance. In most applications, the number of classes is unknown. Here we propose a method for choosing the best number of classes and we apply it to a synthetic and a real texture representation problem.

2. Gabor filters and feature extraction

Gabor filters perform a local Fourier analysis and are essentially sine and cosine functions modulated by a Gaussian window. In the complex space these filters are defined as

$$G(x,y,k_x,k_y) = \exp\left\{\frac{-(x-X)^2+(x-Y)^2}{2\sigma^2}\right\}\cdot e^{j(k_x x+k_y y)}, \tag{1}$$

where x, y represent the spatial coordinates while k_x, k_y represent the frequency coordinates. X and Y are the spatial localizations of the Gaussian window. The filter's selectivity in spatial frequency and orientation is given by

$$\omega = 2\pi\sqrt{k_x^2+k_y^2} \quad \text{and} \quad \theta = \arctan\frac{k_x}{k_y}. \tag{2}$$

Since the signals to be processed are sampled, a binomial window is used to get windowed signals with exact finite dimensions and the Discrete Fourier Transform (DFT) is applied (Neyt et al., 1996). The mathematical expression of the binomial window with dimension $(N+1)\times(M+1)$ (N and M even) is

$$W^2(n,m) = \frac{1}{2^{(N+M)}} C_N^{((N/2)+n)} C_M^{((M/2)+m)} \tag{3}$$

and the DFT basis functions are

$$\sin 2\pi\left(\frac{kn}{N+1}+\frac{lm}{M+1}\right) \quad \text{and} \quad \cos 2\pi\left(\frac{kn}{N+1}+\frac{lm}{M+1}\right),$$

where $n=-N/2,\ldots,N/2$, $m=-M/2,\ldots,M/2$ represent the discrete spatial coordinates while $k=-K/2,\ldots,K/2$ and $l=-L/2,\ldots,L/2$ respresent the discrete frequency coordinates. The filter's central frequency and orientation become

$$\omega = 2\pi\sqrt{\left(\frac{k}{N+1}\right)^2+\left(\frac{l}{M+1}\right)^2} \tag{4}$$

and

$$\theta = \arctan\frac{k}{N+1}\frac{M+1}{l}. \tag{5}$$

The number of filters is given by

$$\frac{(K+1)\times(L+1)-1}{2}+1.$$

Fig. 1 shows some Gabor filter functions obtained for a 31×31 binomial window and the following five discrete values $\{-2,-1,0,1,2\}$ taken by k and l. This gives 13 filters, each of them is represented by the sine and cosine components. Fig. 2 shows how these components are ordered.

Gabor filter responses are determined by convolution of the input image with functions having the forms given above. The convolution output at each point is the information about the spatial relationship between pixels and their neighborhoods.

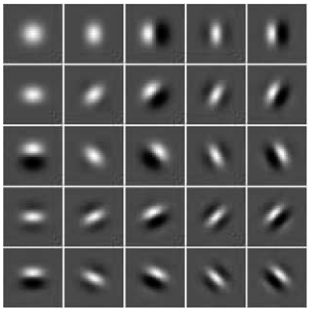

Fig. 1. Bank of Gabor filters (grey = 0, white = positive values, black = negative values).

$C_{0,0}$	$C_{0,1}$	$S_{0,1}$	$C_{0,2}$	$S_{0,2}$
$C_{1,0}$	$C_{1,1}$	$S_{1,1}$	$C_{1,2}$	$S_{1,2}$
$S_{1,0}$	$C_{-1,1}$	$S_{-1,1}$	$C_{-1,2}$	$S_{-1,2}$
$C_{2,0}$	$C_{2,1}$	$S_{2,1}$	$C_{2,2}$	$S_{2,2}$
$S_{2,0}$	$C_{-2,1}$	$S_{-2,1}$	$C_{-2,2}$	$S_{-2,2}$

Fig. 2. Ordering of Gabor filters $k, l = -2, \ldots, 2$: $S_{k,l}$ and $C_{k,l}$ are, respectively, their sine and cosine terms.

The feature extraction phase results in a set of feature images obtained by computing local 'energy' (Kruizinga and Petkov, 1999) from each Gabor filter response. If I is the textured image, the local 'energy' at position (n, m) is given by

$$E_{k,l}(n,m) = [(C_{k,l} \otimes I)(n,m)]^2 + [(S_{k,l} \otimes I)(n,m)]^2. \tag{6}$$

Here, $\otimes$ denotes the convolution and k, l the frequency coordinates.

Let us assume P number of filters; the vector represented by $\vec{x} = \langle E_{0,0}(n,m), \ldots, E_{k,l}(n,m), \ldots \rangle$ constitutes the P-dimensional feature vector which characterizes a given pixel (n, m) in the image. Fig. 4 illustrates the effect of the application of the Gabor filter bank (given in Fig. 1) on an input textured image (Fig. 3).

3. Classification

Many algorithms have been developed for supervised and unsupervised classification. In supervised classification, training sets are needed whereas unsupervised classification classifies images automatically by finding clusters in the feature space. One of the unsupervised data clustering methods is the hard k-means clustering algorithm. It assigns each sample (feature vector) to one and only one of the clusters. This method assumes that boundaries between clusters are well defined. The model does not reflect real data where samples are in general mixed. In fuzzy c-means algorithm (Bezdek and Pal, 1992), unlike the k-means algorithm, samples belong to all clusters with various membership degrees. Membership degree u_{ij} is defined as a function of the distance $d(\vec{x}_j, \vec{c}_i)$ between sample $\vec{x}_j$ and the ith-cluster center $\vec{c}_i$. The fuzzy c-means may be seen as a generalization of the k-means method with membership values in the interval $[0, 1]$ rather than in the set $\{0, 1\}$. The algorithm is an iterative procedure to minimize the following objective function with respect to fuzzy membership u_{ij} and cluster center $\vec{c}_i$:

$$J_m = \sum_{i=1}^{C} \sum_{j=1}^{n} (u_{ij})^m d^2(\vec{x}_j, \vec{c}_i), \tag{7}$$

where $d^2(\vec{x}_j, \vec{c}_i) = (\vec{x}_j - \vec{c}_i)^{\mathrm{T}} \sum_i^{-1} (\vec{x}_j - \vec{c}_i)$ is the Mahalanobis distance with $\sum_i$ being the covariance matrix of samples in cluster i. C is the number of clusters or classes, n is the number of samples and m $(m > 1)$ is the fuzziness index.

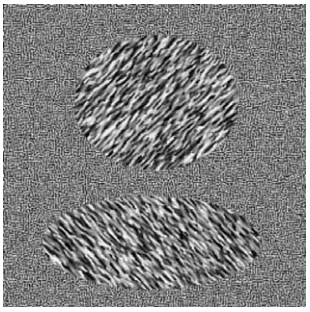

Fig. 3. Synthetic textured image.

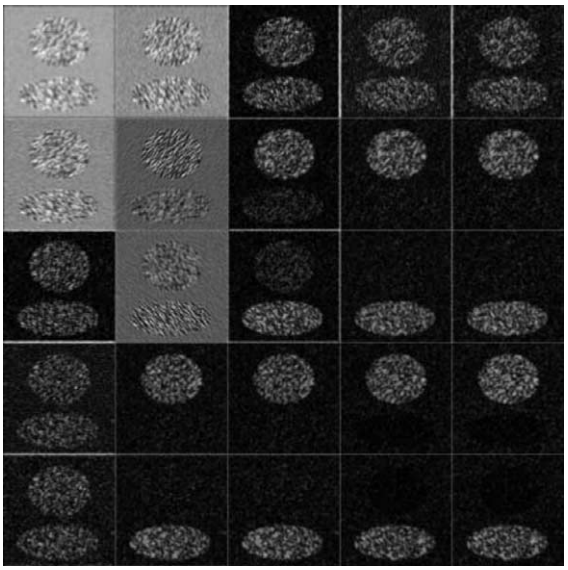

Fig. 4. Gabor filter responses of the textured image.

The algorithm is executed in the following steps:

1. For $i = 1, 2, \ldots, C$ and $j = 1, 2, \ldots, n$ initialize (randomly) u_{ij} such that
$$\sum_{i=1}^{C} u_{ij} = 1. \tag{8}$$
2. Compute u_{ij} and $\vec{c}_i$ using
$$u_{ij} = \left(\frac{1}{d^2(\vec{x}_j, \vec{c}_i)}\right)^{1/(m-1)} \Bigg/ \sum_{i=1}^{C} \left(\frac{1}{d^2(\vec{x}_j, \vec{c}_i)}\right)^{1/(m-1)}$$
$$\text{and } \overrightarrow{c_i} = \frac{\sum_{j=1}^{n} (u_{ij})^m \vec{x}_j}{\sum_{j=1}^{n} (u_{ij})^m}. \tag{9}$$
3. Repeat step 2 until the value of J_m (Eq. (7)) is no longer decreasing.

To get a classified image, the fuzzy partition is made hard by assigning a particular sample to the cluster to which it has the highest membership value.

4. Classification validity

Classification of data should be of high quality, i.e., all samples should have a large membership degree for at least one cluster. This problem is related to how many classes there are in the data. In fuzzy c-means algorithm, the number of clusters is required though in many applications this information is unknown. A method for measuring performance is needed to compare the goodness of different classification results. Gath and Geva (1989) have defined an 'optimal partition' of the data into subgroups as

1. Clear separation between the resulting clusters.
2. Minimum volume of the clusters.
3. Maximum number of data points concentrated around the cluster center.

In the literature, this is known as cluster validity problem; there exist a wide variety of cluster validity parameters. Bezdek (1973) has designed the partition coefficient (PC) to measure the amount of overlap between clusters:

$$\mathrm{PC} = \frac{1}{n} \sum_{j=1}^{C} \sum_{j=1}^{n} (u_{ij})^2. \tag{10}$$

The closer this value is to one the better the data are classified. The drawbacks of this coefficient are first, its sensitivity to the values of cluster number C and second, its ignorance of data geometrical structure. Gath and Geva (1989) have proposed the partition density (PD) more related to the geometry of the data set. The method accounts for variability in cluster shapes and the number of data points in each of the subsets:

$$\mathrm{PD} = \frac{S}{\mathrm{FHV}} \tag{11}$$

where $S = \sum_{i=1}^{C} \sum_{j=1}^{n} (u_{ij})$ is the fuzzy cardinality of data set and $\mathrm{FHV} = \sum_{i=1}^{C} [\det(\sum_i)]^{1/2}$ is the fuzzy hyper-volume of data set.

With this criterion, good performance of the classification is achieved for the higher value of the partition density according to a given number of classes. As we will see in practice, this approach does not work well. Indeed, this parameter is only sensitive to well compact substructures in the data set and does not take the overlapping between them into account. Consequently, some over-segmented results give a higher partition density value. To avoid this problem, Xie and Beni (1991) have suggested a validity function which measures the compactness and separation (CS) of a fuzzy partition:

$$\mathrm{CS} = \frac{\sum_{i=1}^{C} \sum_{j=1}^{n} (u_{ij})^2 d^2(\vec{x}_j, \vec{c}_i)}{n \times (d_{\min})^2} = \frac{J_2}{n \times (d_{\min})^2}, \tag{12}$$

where J_2 is the previous objective function (Eq. (7)) defined for the fuzzy clustering algorithm and $d_{\min}$ is the minimum distance between cluster centers. The smallest CS indicates a valid optimal partition of the data set. This cluster validity coefficient seems very attractive, but as pointed out by the authors, the minimization process is influenced by the monotonical decrease of J_2.

For this work, we have defined a cluster validity parameter which is similar to the previous compactness and separation function. To avoid the monotonical decreasing behavior, the compactness

coefficient J_2 is replaced by the partition density PD (Eq. (11)) and a resemblance function r (Bloch, 1999) is used as separation measurement between clusters. This function is based on fuzzy union and intersection derived from the fuzzy sets theory introduced by Zadey (1965):

$$r = \frac{f(A \cap B)}{f(A \cup B)}, \tag{13}$$

where A and B are two fuzzy sets; $f(X)$ is the fuzzy cardinality of a set X. The intersection $A \cap B$ is the largest fuzzy set which is contained in both A and B; the union $A \cup B$, as in the case of the intersection, is the smallest fuzzy set containing both A and B. Using sample membership degrees $u_j(A)$ and $u_j(B)$ related to the fuzzy sets A and B, the resemblance function is defined as

$$r = \frac{\sum_{j=1}^{n} \mathrm{Min}[u_j(A), u_j(B)]}{\sum_{j=1}^{n} \mathrm{Max}[u_j(A), u_j(B)]}. \tag{14}$$

The new definition of compactness and separation coefficient is

$$n\mathrm{CS} = \frac{\mathrm{PD}}{\max(r)}. \tag{15}$$

The factor $\max(r)$ corresponds to the maximum resemblance value measured between two clusters. This normalized factor always takes a value close to zero as soon as the clusters are disjoint; the higher resemblance value is close to one. It can also be interpreted as a punishing factor applied to the partition density PD to avoid the over-segmentation problem.

With this definition, the procedure to select the best number of classes is to cluster the data set for many different number of classes; the best one should give the maximum nCS index.

5. Experiments

5.1. Synthetic images

For experimental results, we present first a visual evaluation of Gabor filters in texture characterization and classification. To do this, we use two synthetic 256×256 textured images, one containing three Gaussian Markov Random Field (GMRF) textures (Fig. 5) and the other containing five textures from the Brodatz album (Brodatz, 1966) (Fig. 7). As the number of texture categories is known for these images, we also present the efficiency of the method proposed for classification validity measure.

To get classification results for these two synthetic images assuming the correct number of classes, 13 Gabor filters are computed with an 11×11

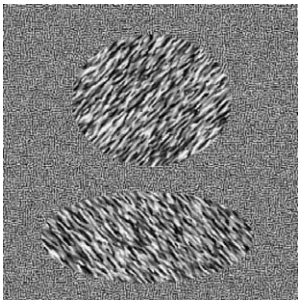

Fig. 5. Synthetic GMRF image.

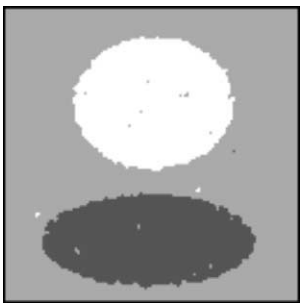

Fig. 6. Classification result.

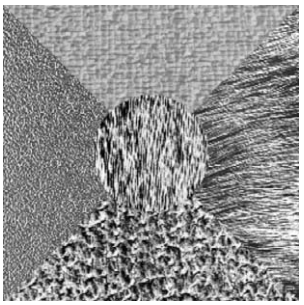

Fig. 7. Brodatz texture image.

binomial window and 5 discrete values of frequency coordinates $k, l \{-2, -1, 0, 1, 2, \}$ (empirically determined). The central frequency and orientation of each filter can be easily calculated from Eqs. (4) and (5). We see that the three textures of GMRF image (Fig. 6) and the five textures from the Brodatz album are successfully discriminated (Fig. 8).

These results are used to discuss the efficiency of the method proposed in this work for the classification validity measure. We present the behavior of the validity functions discussed in the previous paragraph. For these two synthetic images, we plot successively in Figs. 9 and 10 the partition coefficient PC and partition density PD. As we can see, the first validity function PC decreases monotonically and is not useful for selecting the best number of classes. The PD function detects successfully 5 classes for the Brodatz image but presents a maximum at 4 for the GMRF image. This means that, according to density criterion, this number of classes is a best candidate for the classification process but Fig. 11 shows the over-segmentation obtained with 4 as the number of classes.

To avoid this over-segmentation problem, we have proposed to use the resemblance factor $\max(r)$ as punishing coefficient for PD function. Fig. 12 shows the behavior of this factor applied to the test images. The curves present a significant knee at 3 and 5. This means that beyond these values, clusters with high resemblance appear in the classification process. In Fig. 13, the proposed compactness and separation function gives the optimal number of clusters corresponding for the two test images.

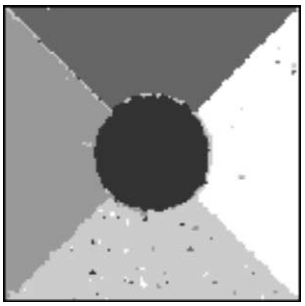

Fig. 8. Classification result.

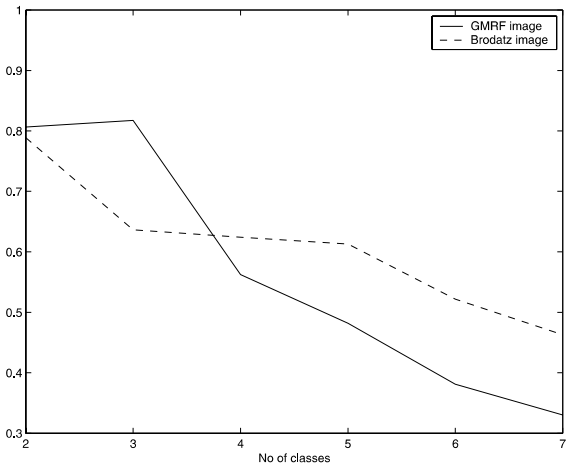

Fig. 9. Partition coefficient.

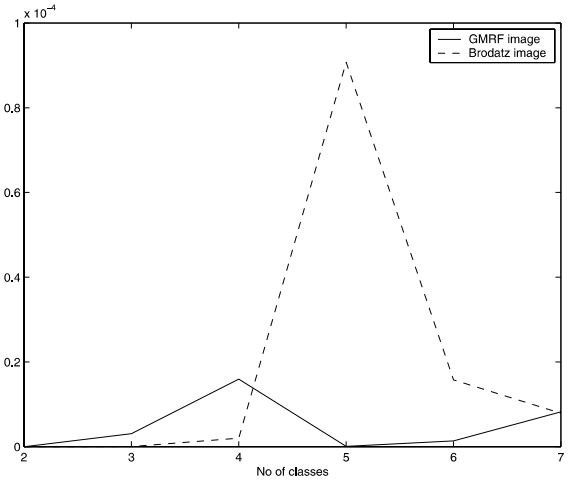

Fig. 10. Partition density.

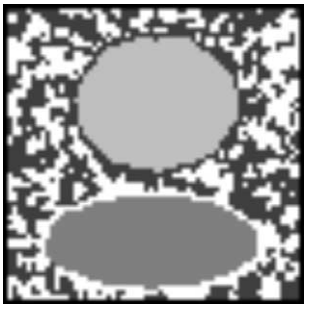

Fig. 11. Four classes over-segmentation of GMRF image.

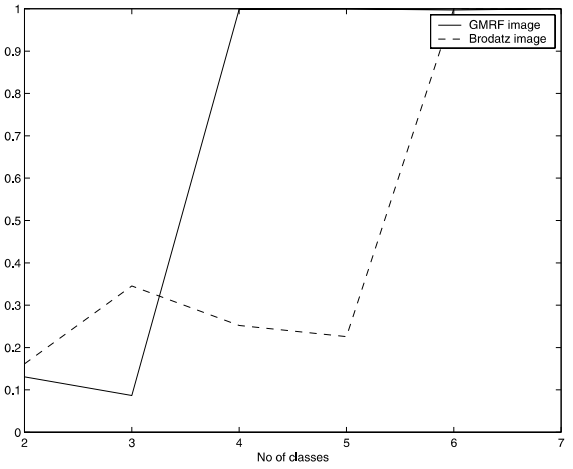

Fig. 12. Resemblance function.

5.2. Real world problem

We now apply this texture classification method to a grey-scale image (Fig. 14) obtained from a section of a color IR image. The images were taken in November 1998 during an airborne minefields survey in Mozambique (Yvinec et al., 1999). In the surveyed area, minefields are homogeneous regions with no human activity inside and surrounded by agricultural fields. Since the vegetation in these minefields is different from the vegetation outside, texture based classification is a good approach for the interpretation of this image. Unfortunately, exact class maps or texture models are not available. Thus, the use of the proposed cluster validity parameter will help us to find the optimal class number which maximizes the final classification accuracy.

Gabor filters are computed with an 11×11 binomial window and 5 discrete values of frequency coordinates $k, l \{-2, -1, 0, 1, 2\}$ (empirically determined). We have used only 9 features selected from the 13 feature images. The feature selection scheme is based on a simple method which consists in sorting the feature images based on their amount of energy and pick up as many features as needed to achieve 95% of the total energy.

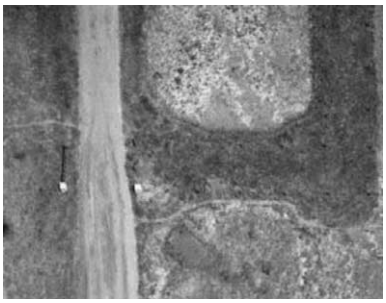

Fig. 14. Aerial image of a minefield area in Mozambique.

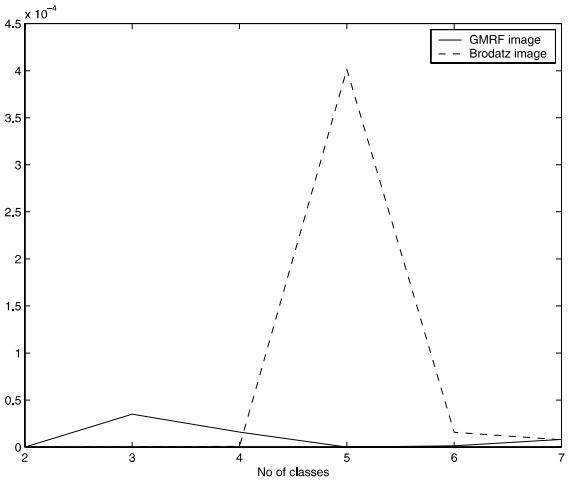

Fig. 13. Compactness and separation function.

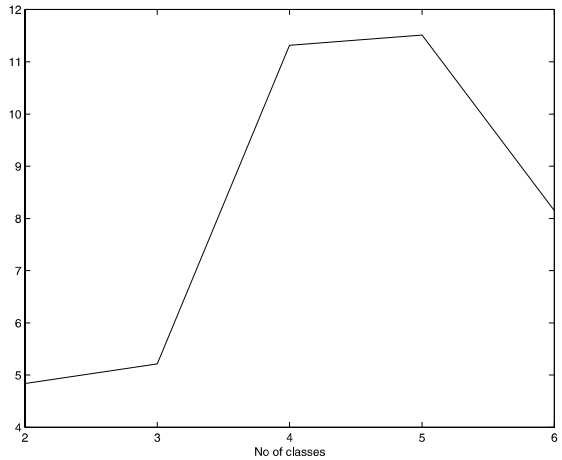

Fig. 15. Compactness and separation function (nCS) for the aerial image.

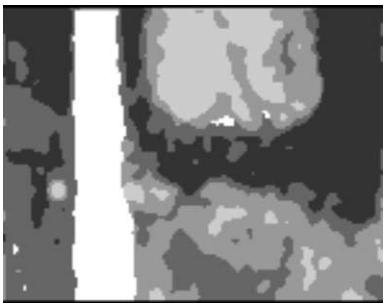

Fig. 16. Classification in 5 classes.

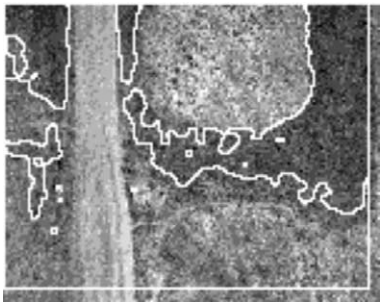

Fig. 17. Minefield region detected.

The optimal number of clusters that we find for this image is 5 (see Fig. 15) and the classification result is presented in Fig. 16. As we can see in Fig. 17, the dark area corresponding to the suspected minefield is determined and the other types of vegetation as well.

6. Conclusions

A fuzzy clustering approach to textured image classification has been presented. The texture features are extracted using a set of Gabor filters with different frequencies and orientations.

The fuzzy c-means algorithm has been successfully used for discriminating different types of textured image but the drawback is that one has to specify the number of clusters. We thus discussed the use of cluster validity parameters. A modification of compactness and separation validity function is proposed as index to estimate the optimal number of texture categories which has proven adequate for texture discrimination.

Acknowledgements

The authors are grateful to colleagues: Dr. V. Lacroix for the helpful and encouraging discussions during the preparation of this paper and X. Neyt who develops the Gabor filter tools. They also would like to thank the International Institute for Aerospace Survey and Earth Sciences (ITC, The Netherlands) for providing the minefield aerial image in the frame of European Pilot Project entitled: Airborne Minefield Detection.

References

Bezdek, J.B., 1973. Cluster validity with fuzzy sets. J. Cybern. 3, 58–73.

Bezdek, J.C., Pal, S.K., 1992. Fuzzy Models for Pattern Recognition. IEEE Press, New York.

Bloch, I., 1999. On fuzzy distance and their use in image processing under imprecision. Pattern Recognition 32 (11), 1873–1895.

Bovik, A.C., Clarke, M., Geisler, W.S., 1990. Multichannel texture analysis using localized spatial filters. IEEE Trans. Pattern Anal. Machine Intell. 12, 55–73.

Brodatz, P., 1966. Textures: A Photographic Album for Artists and Designers. Dover, New York.

Cross, G.R., Jain, A.K., 1983. Markov random field texture models. IEEE Trans. Pattern Anal. Machine Intell. 5, 25–39.

Gath, I., Geva, A.B., 1989. Unsupervised optimal fuzzy clustering. IEEE Trans. Pattern Anal. Machine Intell. 11 (7), 773–781.

Haralick, R.M., 1979. Statistical and structural approaches to texture. Proc. IEEE 67, 786–804.

Kruizinga, P., Petkov, N., 1999. Nonlinear operator for oriented texture. IEEE Trans. Image Process. 8 (10), 1395–1407.

Neyt, X., Acheroy, M., Lemahieu, I., 1996. Directional adaptive image restoration. In: Proc. Internat. Workshop on Image and Signal Processing IWISP'96, November.

Randen, T., Husoy, J.H., 1999. Filtering for texture classification: a comparative study. IEEE Trans. Pattern Anal. Machine Intell. 21 (4), 291–310.

Xie, X.L., Beni, G., 1991. A validity measure for fuzzy clustering. IEEE Trans. Pattern Anal. Machine Intell. 13 (8), 841–847.

Yvinec, Y., Druyts, P., Lacroix, V., Ouaghli, Y., Idrissa, M., 1999. Airborne minefield detection: pilot project rma/sic final report. Technical Report, Royal Military Academy/ Signal and Image Centre, Avenue de la Renaissance 30, B-1000 Brussels.

Zadey, L.A., 1965. Fuzzy sets. Inf. Control 8, 338–353.